

# Thermodynamics of Block Copolymer Solutions As Compared with the Corresponding Homopolymer Solutions: Experiment and Theory

Xiaopeng Xiong,<sup>†,‡</sup> John Eckelt,<sup>‡,§</sup> Lina Zhang,<sup>†</sup> and Bernhard A. Wolf<sup>\*,‡</sup>

<sup>†</sup>Department of Materials Science and Engineering, College of Materials, 361005 Xiamen, China, <sup>‡</sup>Institut für Physikalische Chemie der Johannes Gutenberg Universität and Materialwissenschaftliches Forschungszentrum, Universität Mainz, Welder-Weg 13, D-55099 Mainz, Germany, <sup>§</sup>WEE-Solve GmbH, Auf der Burg 6, 55130 Mainz, Germany, and <sup>†</sup>Department of Chemistry, Wuhan University, 430072 Wuhan, China

Received July 6, 2009; Revised Manuscript Received August 13, 2009

**ABSTRACT:** The interaction of butadiene–styrene block copolymers of different molecular architecture with tetrahydrofuran (THF) was studied by vapor pressure and light scattering experiments in the temperature range from 25 to 55 °C. The thus obtained Flory–Huggins interaction parameters,  $\chi$ , as a function of  $\phi$ , the volume fraction of the polymers, were compared with that of the corresponding homopolymers in the same solvent. The results are very similar for all block copolymers (diblock, triblock and star-shaped, butadiene in the center) and for all temperatures. In contrast to the  $\chi(\phi)$  curves of the homopolymers, which are always located above their tangents, the dependencies for the block copolymers exhibit a maximum in the range of moderate polymer concentrations, where the heats of dilution are close to athermal in the range of low  $\phi$  values but become pronouncedly endothermal for high  $\phi$  values. These findings can be well modeled by an approach considering the phenomena of chain connectivity and conformational relaxation of polymers, if one accounts for the unfavorable interactions between the monomeric units of the different blocks.

## 1. Introduction

This contribution aims at an improved understanding of the thermodynamic behavior of block copolymers in solution. Progress in this area would be highly welcome in view of the practical<sup>1–4</sup> and theoretical importance<sup>2,5,6</sup> of this class of macromolecules. One of the reasons, why such polymers are so interesting lies in their microphase separation<sup>7–9</sup> and in the corresponding formation of particular structures at high polymer concentrations.<sup>10,11</sup> For the present work, we are, however, not worrying about these phenomena; they do not constitute any obstacle for the determination of Flory–Huggins interaction parameters, as long as the systems are in thermodynamic equilibrium. From the fact that we measure the same vapor pressure for a given solution, irrespective of whether its composition is reached by the addition or removal of solvent, and in view of the good reproducibility of the data obtained in independent measurements, we conclude that this condition is well fulfilled for the present system.

By means of the investigation communicated here, we wanted above all to answer the question as to how the polymer solvent interaction of the block copolymers of different molecular architecture compares with that of the corresponding homopolymers and the same solvent. The well-defined polymer samples required for that purpose were synthesized and characterized as already described.<sup>12</sup> The experimental work consists primarily of vapor pressure and light scattering measurements. The theoretical analysis uses a modified Flory–Huggins theory, accounting for the effects of chain connectivity and conformational relaxation of a polymer in solution.<sup>13,14</sup>

## 2. Experimental Section






**2.1. Materials.** Samples of linear polybutadiene (PB) were kindly donated by Lanxess Deutschland GmbH.

\*Corresponding author. E-mail: bernhard.wolf@uni-mainz.de.

Poly(styrene-*block*-butadiene) copolymers of different molecular architectures were polymerized anionically according to literature.<sup>12</sup> The linear diblock copolymer, the linear triblock copolymer with polybutadiene the inner block ((SB)2), and the star-shaped four-arm copolymer with polybutadiene as the inner blocks ((SB)4), were fractionated by using the continuous spin fractionation (CSF) method<sup>12</sup> to increase the molecular uniformity. The schematic molecular structures, the weight-average molecular weight ( $M_w$ , from light scattering, polydispersity indices ( $d = M_w/M_n$  from GPC), butadiene content, vinyl content and *cis*-butadiene content of the polymers (from <sup>1</sup>H NMR measurements<sup>12</sup>) are listed in Table 1. Tetrahydrofuran (THF) was analytical grade and was purchased from Fluka (Buchs, Switzerland). The densities of the block copolymers were obtained by measuring the densities of their solutions in THF as a function of composition by means of the density meter DMA 48, from Anton Paar, Austria, and extrapolating these data to the pure state. The densities of polybutadiene stem from pycnometric measurements. All results are collected in Table 2, together with the numbers of segments of the polymers calculated defining the size of the segments via the solvent THF.

**2.2. Apparatuses and Procedures.** *Headspace Sampling–Gas Chromatography (HS–GC).* HS–GC measurements have been carried out with an apparatus consisting of a headspace-sampler and a normal gas chromatograph, as already described in detail.<sup>17,18</sup> The pneumatically driven thermostated headspace sampler (Dani HSS 3950, Milan, Italy) transfers a constant amount of the gas phase (in equilibrium with the liquid) and injects it into a gas chromatograph (Shimadzu GC 14B, Kyoto, Japan). This procedure gives access to the amounts of the volatiles in a constant volume of vapor phase, which is in thermodynamic equilibrium with the liquid. The amount of solvent contained in the sample volume, proportional to the vapor pressure, is detected by a flame ionization detector (Shimadzu, Chromatopac C-R6A, Kyoto, Japan). The injector

Table 1. Characteristic Polymer Data<sup>a</sup>

	PB	PS	SB	(SB)2	(SB)4
molecular architecture					
$M_w$ (kg/mol)	101	29.8	109	85.5	220
$d = M_w/M_n$	1.11	1.10	1.17	1.12	1.11
butadiene (mol %)	100	-	76.7	74.2	74.4
vinyl content (mol %)	10.0	-	4.7	7.3	7.4
cis content (mol %)	38.2	-	5.1	7.4	7.3

<sup>a</sup> Key:  : polybutadiene,  : polystyrene

Table 2. Densities ( $\rho$ ) and Numbers of Segments ( $N$ ), Where the Solvent Defines the Size of a Segment<sup>a</sup>

	$t = 25\text{ }^\circ\text{C}$		$t = 40\text{ }^\circ\text{C}$		$t = 55\text{ }^\circ\text{C}$	
	$\rho$ (g/mL)	$N = N_B + N_S$	$\rho$ (g/mL)	$N = N_B + N_S$	$\rho$ (g/mL)	$N = N_B + N_S$
THF <sup>15</sup>	0.881	1	0.866	1	0.852	1
PB <sup>16</sup>	0.895	940	0.887	930	0.878	920
SB	0.956	1066 + 324	0.955	1051 + 319	0.957	1035 + 315
(SB)2	0.979	794 + 276	0.970	779 + 271	0.963	764 + 266
(SB)4	0.965	2076 + 714	0.961	2039 + 701	0.955	2001 + 689

<sup>a</sup> The  $N$  value of the block copolymers is the sum of the block segments  $N_B$  and  $N_S$ .

Table 3. Characteristic Parameters of Eq 17 and Refractive Index Increments  $dn/dc$  for the System THF/PB

	25 °C	40 °C	55 °C
$dn/dc$ (mL/g)	0.130	0.138	0.143
$\chi_o$	$0.399 \pm 0.000$	$0.401 \pm 0.000$	$0.401 \pm 0.000$
$\xi\lambda$	$0.371 \pm 0.001$	$0.460 \pm 0.019$	$0.495 \pm 0.029$
$\nu$	$0.237 \pm 0.001$	$0.291 \pm 0.005$	$0.297 \pm 0.006$
$\tau$	0.000	0.000	0.000

Table 4. Parameters of Eq 17 for the System THF/PS

	20 °C	40 °C	60 °C
$\chi_o$	$0.419 \pm 0.000$	$0.417 \pm 0.000$	$0.416 \pm 0.000$
$\xi\lambda$	$1.260 \pm 0.050$	$1.180 \pm 0.070$	$1.110 \pm 0.050$
$\nu$	$0.324 \pm 0.116$	$0.310 \pm 0.016$	$0.295 \pm 0.012$
$\tau$	0.000	0.000	0.000

was kept at 80 °C, while the column and the detector temperature was 100 °C. No corrections for the nonideality of the gas had to be made.

**Light Scattering (LS).** LS measurements were performed in THF at different temperatures with a modified (SLS, G. Bauer, Freiburg, Germany) static light scattering (SLS) apparatus Fica 50 (Sofica, Paris) using an unpolarized laser light of 632.8 nm and covering angles between 20° and 145°. Prior to the measurements, the polymer solutions with concentrations ranging from 1 to 10 g/L were filtered through a 0.45  $\mu$ m membrane filter (Millipore) directly into the thoroughly cleaned optical cells (Hellma, Muellheim, Germany) and thermostated in the light-scattering apparatus for 20 min. The differential refractive index increments ( $dn/dc$ , collected in Tables 3–6) required for that purpose stem from measurements on a Bodmann differential refractometer.<sup>19</sup> The automatically registered intensities of the scattered light were

Table 5. Parameters of the Redlich–Kister Equation (Eq 11) Used to Model  $\chi(\phi)$  for the System THF/SB at 25 °C Setting  $f = 2$ 

$a$	$b$	$c$	$d$	$k$
$0.247 \pm 0.014$	$0.185 \pm 0.050$	$-0.034 \pm 0.023$	$-0.397 \pm 0.061$	$0.247 \pm 0.014$

Table 6. Characteristic Parameters of Eq 17 and Refractive Index Increments  $dn/dc$  for the System THF/SB

	25 °C	40 °C	55 °C
$dn/dc$ (mL/g)	0.151	0.158	0.163
$\chi_o$	$0.420 \pm 0.000$	$0.371 \pm 0.000$	$0.371 \pm 0.000$
$\xi\lambda$	$-0.876 \pm 0.031$	$-1.022 \pm 0.175$	$-1.022 \pm 0.096$
$\nu$	$0.684 \pm 0.008$	$0.651 \pm 0.016$	$0.651 \pm 0.017$
$\tau$	$1.705 \pm 0.020$	$1.841 \pm 0.094$	$1.841 \pm 0.039$

evaluated in Zimm plots using a program provided by the producer of the SLS instrument.

### 3. Theoretical Background

According to the Flory–Huggins theory the following expression for the difference in the chemical potential of the solvent ( $\Delta\mu_1$ ) in a polymer solution as compared with the pure solvent holds true

$$\frac{\Delta\mu_1}{RT} = \ln(1 - \phi) + \left(1 - \frac{1}{N}\right)\phi + \chi\phi^2 \quad (1)$$

$R$  is the gas constant,  $T$  the absolute temperature,  $\phi$  the volume fraction of polymer,  $N$  the number of segments of a polymer defined as the ratio of the molar volume of the polymer to the solvent, and  $\chi$  the Flory–Huggins interaction parameter. The chemical potentials can be measured by means of several different methods based on phase equilibria. Equilibrium vapor pressures

are one important source of information. In case gas imperfections can be neglected, one can write

$$\Delta\mu_1 = \ln \frac{p_1}{p_{1,0}} \quad (2)$$

where  $p_{1,0}$  is the vapor pressure of the pure liquid and  $p_1$  the vapor pressure above the solutions. With this relation and eq 1 we obtain the following expression for the Flory–Huggins interaction parameter

$$\chi = \frac{\ln \frac{p_1}{p_{1,0}} - \ln(1 - \varphi) - \left(1 - \frac{1}{N}\right)\varphi}{\varphi^2} \quad (3)$$

As documented by eqs 3 and 2, the Flory–Huggins interaction parameter constitutes a measure for chemical potential of the solvent. In the original theory it was meant to have an immediate physical meaning; because of the normalization of the segment molar Gibbs energies of dilution to the probability  $\varphi^2$  of an added solvent molecule to be inserted between two contacting polymer segments. This illustrative interpretation does, however, rarely hold true. Even for simple homopolymer solutions in single solvents, it fails in the region of high dilution, because the overall polymer concentration becomes meaningless for the number of intermolecular contacts between polymer segments. Similarly it is impossible to assign the  $\chi$  values obtained for the block copolymer solutions to individual molecular processes because of the strong preferential interactions and the occurrence of microphase separation at higher polymer concentrations. Nevertheless the knowledge of  $\chi(\varphi)$  is indispensable for the thermodynamic description of such systems. This information can be converted to integral interaction parameters  $g$  (cf. eq 8) and gives access to the calculation of macrophase separation (e.g., via a direct minimization of the Gibbs energy of the systems) and to the chemical potentials of the polymer (cf. eq 10).

It is meanwhile well established that composition independent Flory–Huggins interaction parameters are rare exceptions. The simplest manner to account for that observation is the representation of  $\chi(\varphi)$  in form of a series expansion. At constant temperature, this relation reads

$$\chi = \chi_0 + \chi_1\varphi + \chi_2\varphi^2 + \dots \quad (4)$$

where the parameters  $\chi_1, \chi_2, \dots$  are temperature dependent constants.

The fact that  $\chi$  is in the general case composition dependent has several important consequences. First of all it is obvious that different experimental methods must be combined to determine  $\chi$  within the entire range of composition. For the present work, we have therefore performed light scattering measurements in addition to the vapor pressure measurements. These experiments yield information on the thermodynamic behavior of dilute polymer solutions. The obtained data were evaluated according to

$$\frac{Kc}{\Delta R_\theta} = \frac{1}{M_w} + 2A_2c + 3A_3c^2 + \dots \quad (5)$$

where  $c$  is the polymer concentration in mass/volume,  $\Delta R_\theta$  is the excess Rayleigh ratio,  $K$  is a constant containing the refractive index increment, and the  $A_i$  are the osmotic virial coefficients, which are related to the coefficients of the series expansion of  $\chi$  formulated in eq 4 by

$$\chi_0 = \frac{1}{2} - \rho_2^2 \bar{V}_1 A_2 \quad (6)$$

and

$$\chi_1 = \frac{1}{3} - \rho_2^3 \bar{V}_1 A_3 \quad (7)$$

In these relations  $\rho_2$  is the density of the polymer and  $\bar{V}_1$  is the partial molar volume of the solvent.

Another important consequence of  $\chi(\varphi)$  lies in the necessity to distinguish three different interaction parameters for the present polymer solutions. In addition to  $\chi$ , based on the chemical potential of the solvent and quantifying the effects upon dilution, we need to introduce an integral interaction parameter  $g$  and a differential interaction parameter  $\xi$ , defined in terms of the chemical potential of the polymer. The following interrelations hold true

$$g = \frac{1}{\varphi_1} \int_0^{\varphi_1} \chi \, d\varphi_1 \quad (8)$$

where  $\varphi_1 = 1 - \varphi$  or conversely

$$\chi = g - (1 - \varphi) \frac{\partial g}{\partial \varphi} \quad (9)$$

The differential interaction parameter  $\xi$ , defined in terms of the chemical potential of the polymer is obtained from  $g$  as

$$\xi = g + \varphi \frac{\partial g}{\partial \varphi} \quad (10)$$

**3.1. Redlich–Kister.** Equation 11 is a special form of the series expansion of eq 4

$$\chi = a + b(f\varphi - 1) + c(f\varphi - 1)^2 + d(f\varphi - 1)^3 + k(f\varphi - 1)^4 + \dots \quad (11)$$

where  $a, b, c, d, f$ , and  $k$  are adjustable parameters. This relation<sup>20</sup> is widely used by engineers in the pharmaceutical field,<sup>21</sup> to model phase diagrams of alloys<sup>22</sup> and multinary mixtures.<sup>23,24</sup>

**3.2. Chain Connectivity and Conformational Relaxation.** In contrast to most other expressions used for the modeling of the composition dependence of the Flory–Huggins interaction parameter, this approach accounts explicitly for non-random mixing. For the present systems, it is of utmost importance to model the deviations of local concentrations from the compositions expected from the composition of the mixture in view of the incompatibility of the homopolymer blocks leading to microphase separation.

The central equation of the approach was obtained by conceptually subdividing the dilution process into two separate steps.<sup>13,14</sup> New contacts between the components are formed in the first step, keeping their conformation constant. This process does not yet result in equilibria; it is only during the second step, the conformational rearrangement of the components, that the minimum in the Gibbs energy of the system is reached.

$$\chi = \frac{\alpha}{(1 - \nu\varphi)^2} - \zeta\lambda(1 + 2\varphi) \quad (12)$$

The first term of this relation, corresponding to the first step of dilution, correlates to the original Flory–Huggins interaction parameter expression, except for the parameter  $\nu$ , which accounts for the differences in the surface to volume ratio of the polymer segments as compared with this value

for the solvent (defining the size of segments). All effects of nonrandom mixing are contained in the second term, corresponding to the second step of dilution. Chain connectivity (the segments of a given macromolecule cannot be distributed evenly over the entire volume of the system) is one source of nonrandomness and measured by  $\lambda$ , which is on the order of 0.5 for polymer solutions. The preference or avoidance of the components of a mixture for hetero contacts constitutes the other source of deviation from the combinatorial behavior. The parameter  $\zeta$ , quantifying the contributions of molecular rearrangements to  $\chi$ , can be positive or negative; under  $\Theta$  conditions it becomes zero. The parameters  $\zeta$  and  $\alpha$  represent reduced Gibbs energies by their nature; this means that they are made up by enthalpy and entropy contributions as verified experimentally.<sup>25</sup>

Equation 12 has stood the test for many polymer solutions (including random copolymers); however, it failed in the case of aqueous solutions of polysaccharides. For this class of polymers, exhibiting strong intermolecular interactions, it turned out necessary to add an extra term in the expression for the integral interaction parameter  $g$  as formulated in the next equation.

$$g = \frac{\alpha}{(1-\nu)(1-\nu\varphi)} - \zeta\lambda(2+\varphi) + \omega\varphi^2 \quad (13)$$

This relation enabled the quantitative modeling of  $\chi$  ( $\varphi$ ) for water/pullulan<sup>26</sup> and water/dextran.<sup>26</sup> In these cases the special interactions between the solute involve two segments and the insertion of a solvent molecule between *two* contacting segments (belonging to two different polymer molecules) destroys very favorable hydrogen bonds. In other words: The extra contribution to  $g$  is due to the opening of *binary contacts* and implicates a dependence on the square of  $\varphi$  for the last term of eq 13.

With the block copolymers of present interest the situation is different because of the microphase separation induced by the incompatibility of the blocks. In this case the number of segments required for favorable interactions (more precisely for the avoidance of highly unfavorable contacts to the opposite block) is larger than two. Geometrical considerations suggest that contacts between more than *three* segments belonging to different polymer chains are very unlikely, even in the pure melt. This means that the insertion of a solvent molecule will typically destroy advantageous *ternary contacts* between segments. By analogy to the above reasoning this implies that the extra contribution to  $g$  should depend on the third power of  $\varphi$  in the case of block copolymers, as formulated in eq 14.

$$g = \frac{\alpha}{(1-\nu)(1-\nu\varphi)} - \zeta\lambda(2+\varphi) + \tau\varphi^3 \quad (14)$$

Like  $\omega$ , the parameter  $\tau$  represents a special contribution to the nonrandomness of mixing (absent for ordinary systems) accounting for the pronounced rearrangement of the components after the forced opening of highly favorable contacts. In the following we are testing whether this relation is able to model the experimental findings.

Equation 14 describes how  $g$ , the *integral* interaction parameter, varies with composition, whereas the present experimental information is exclusively given in terms of the *differential* parameters  $\chi$ . Equations 14 and 9 yield the required expression for the Flory–Huggins interaction parameter

$$\chi = \frac{\alpha}{(1-\nu\varphi)^2} - \zeta\lambda(1+2\varphi) + \tau\varphi^2(4\varphi-3) \quad (15)$$

The ability of this approach to account for nonrandom mixing represents a consequence of the conformational relaxation; the rearrangement in the second step of mixing installs thermodynamically preferred molecular neighborhoods and corresponds to the establishment of “quasi-chemical equilibria”.

Equations 12 and 15 simplify to

$$\chi_o = \alpha - \zeta\lambda \quad (16)$$

in the limit of  $\varphi \rightarrow 0$ . The fact that the leading parameters  $\alpha$  and  $\zeta\lambda$  of the approach are related to the second osmotic virial coefficient  $A_2$  via eq 6 turns out to be very helpful for the modeling. Because of the fact that  $A_2$  is normally accessible with great precision and that it constitutes only a modification of the value 0.5 in the equation for  $\chi_o$ , we rewrite eq 15 as

$$\chi = \frac{\chi_o + \zeta\lambda}{(1-\nu\varphi)^2} - \zeta\lambda(1+2\varphi) + \tau\varphi^2(4\varphi-3) \quad (17)$$

and adjust only the three parameters  $\nu$ ,  $\zeta\lambda$  and  $\tau$ . Extensive experimental information for ordinary polymer solutions ( $\tau = 0$ ) has furthermore demonstrated that the parameters  $\alpha$  and  $\zeta\lambda$  are not independent of each other (in agreement with theoretical considerations) but interrelate according to the relation

$$\zeta\lambda = E(2\alpha - 1) \quad (18)$$

where  $E$  is a constant for a given class of polymers. For such systems the number of parameters that need to be adjusted for the modeling is reduced by one; whether eq 18 remains valid for the block copolymer solutions of present interest still needs to be checked.

#### 4. Results and Discussion

This section is organized in the following way. First we report experimental data for the homopolymers corresponding to the copolymer blocks and model their solution behavior in THF on the basis of eq 12. The subsequent section deals with the block copolymers and starts with a discussion of the aptness of the Redlich–Kister equation for the modeling of the experimental data as compared with eq 17, resulting from an extension of the concept of chain connectivity and conformational relaxation to block copolymers. The rest of this part is devoted to the evaluation of the entire experimental material. The concluding third section presents a common analysis of all data and examines the particularities of the block copolymer solutions as compared with ordinary homopolymer solutions.

**4.1. Homopolymers.** The data for the solutions of polybutadiene in THF stem for the present measurements that for the solutions of polystyrene from a recent publication.<sup>27</sup>

*THF/Polybutadiene.* Figure 1 shows the reduced equilibrium vapor pressures of THF above the solutions of polybutadiene (PB) as a function of  $\varphi$ , the volume fraction of PB, for the indicated temperatures; these data stem from HS–GS measurements. For better reading the curves in diagrams of this type are shifted as specified in the graphs.

Flory–Huggins interaction parameters  $\chi$  calculated from vapor pressure data (Figure 1) according to eq 3 and  $\chi_o$ , the limiting value of  $\chi$  in the range of pair interaction, obtained from light scattering data according to eq 6 are in Figure 2 plotted as a function of  $\varphi$  for the indicated temperature.

The characteristic parameters of eq 12 used for the modeling of the system THF/PB are collected in Table 3 together



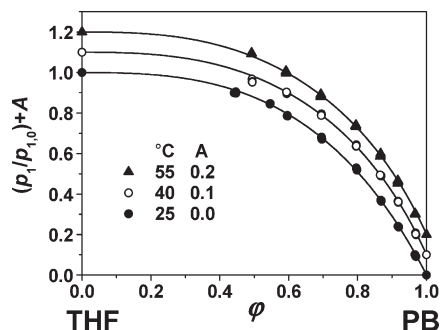


**Figure 1.** Reduced vapor pressures (normalized to the value of the pure solvent THF) as a function of polymer concentration for the system THF/PB. The individual data points were directly obtained from HS–GC measurements, and the curves are calculated by means of the eqs 1 and 2 in combination with eq 17 where the system specific parameters were taken from Table 3. For better differentiation of the symbols and the curves belonging to a certain temperature, the constants  $A$  were added to the ordinate values.

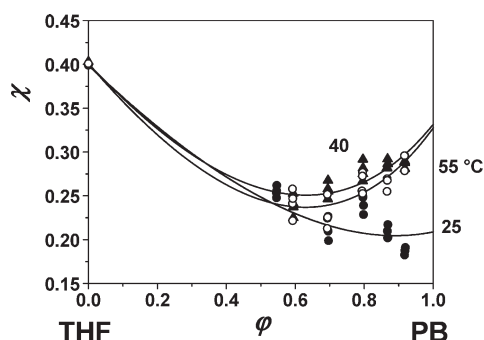


**Figure 2.** Composition dependences of the Flory–Huggins interaction parameter  $\chi$  of the system THF/PB for different temperatures. The individual points were directly calculated from the reduced pressures by means of eq 3. The lines are best fits to these data by means of eq 12.

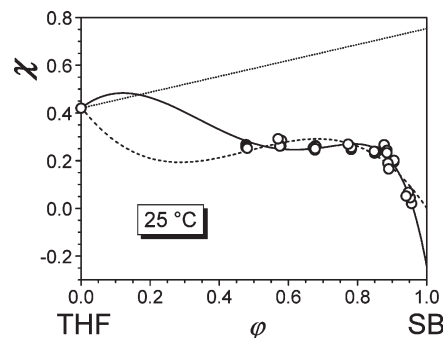
with the refractive index increments required for the light scattering measurements.

**THF/Polystyrene.** The experimental information for this system (Table 4) is taken from the literature.<sup>27</sup>

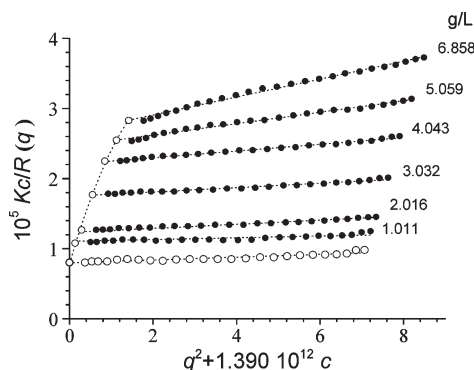
**4.2. Block Copolymers. Evaluation Procedures.** All experimental data concerning the composition dependence of the Flory–Huggins interaction parameter for block copolymer solutions presented in this section demonstrate that the run of these curves is rather complex. That makes the modeling difficult and requires adequate mathematic expressions. Two options are being tested for one of the systems prior to the evaluation of all data, namely the very versatile Redlich–Kister relation (eq 11) and the extension of the concept of chain connectivity and conformational relaxation to block copolymer solutions (eq 15).

Figure 3 shows the results of this modeling for the system THF/SB and 25 °C. The parameters of eq 11 are collected in Table 5, and those of eq 15 are presented in Table 6.

The most obvious difference in the two types of modeling lies in the occurrence of a minimum in  $\chi(\phi)$  on the dilute side in the case of Redlich–Kister (five adjustable parameters if we do not count  $f$ ), in contrast to the modeling according to the present approach (three adjustable parameters, if  $\chi_o$  is excluded as described), which produces a maximum in this composition range. Another dissimilarity of the two options for modeling lies in the considerable better representation of the data at high  $\phi$  values by the latter approach for all nine sets of data. In view of this observation and the lower number of adjustable parameters one is inclined to prefer eq 15 over



**Figure 3.** Modeling of the composition dependence of  $\chi$  for the system THF/SB and 25 °C according to eq 11 (broken curve, parameters of Table 5) and to eq 15 (full curve, parameters of Table 6); the dotted line represents the limiting slope of  $\chi(\phi)$  for infinite dilution in the case of  $A_3 = 0$  (cf. eqs 4 and 7).



**Figure 4.** Zimm plot for the system THF/SB at 25 °C;  $q$  = scattering vector  $A_2 = 1.61 \times 10^{-3} \text{ mol} \cdot \text{mL/g}^2$  and  $A_3 = -0.04 \text{ mol} \cdot \text{mL}^2/\text{g}^3$ .

eq 11. However, to obtain a more solid basis for this choice we have checked, whether the maxima in  $\chi(\phi)$ , i.e. the corresponding set of parameters, may lead to liquid/liquid phase separation. Relevant calculations have shown that the systems remain homogeneous in agreement with the experimental observations made with the present system. This is so because the maximum is not high enough, which means that it may indeed cause macrophase separation (in addition to microphase separation) for sufficiently unfavorable interactions between the two types of monomeric units, as reported in the literature.<sup>28,29</sup>

A further reason to prefer the present approach over Redlich–Kister lies in the initial slope of the composition dependencies of  $\chi$ , which is quantified by  $\chi_1$ . According to eq 7 this parameter should be close to  $1/3$  as long as  $A_3$ , the third osmotic virial coefficient, does not become too large. For the present systems  $A_3$  is actually either very close to zero or even negative as demonstrated for one example in Figure 4. In view of these considerations all further data evaluation is done exclusively on the basis of eq 15.

**THF/SB.** The results of the vapor pressure measurement for the solutions of the diblock copolymer SB are shown in Figure 5. The composition dependence of  $\chi$  obtained from these data and from light scattering experiments yielding  $\chi_o$  is shown in Figure 6 together with the modeling of these results by means of eq 15. The parameters used for this purpose are collected in Table 6. The temperature influences on the interaction parameters remain rather low for this diblock copolymer so that the corresponding curves are shifted for easier reading of the graph.

**THF/(SB)2.** Figure 7 shows the vapor pressures and Figure 8 the Flory–Huggins interaction parameters as a

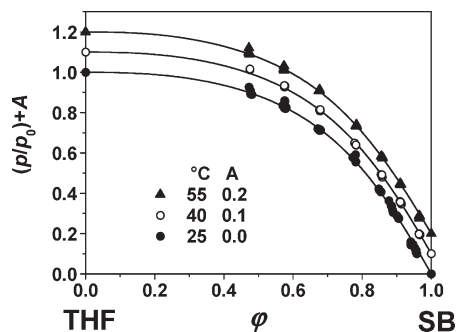


**Figure 5.** Reduced vapor pressures (normalized to the value of the pure solvent THF) as a function of polymer concentration for the system THF/SB. The individual data points were obtained from HS–GC measurements, and the curves are calculated by means of the eqs 1 and 2 in combination with eq 17 where the system specific parameters were taken from Table 6. For better differentiation of the symbols and the curves belonging to a certain temperature, the constants  $A$  were added to the ordinate values.

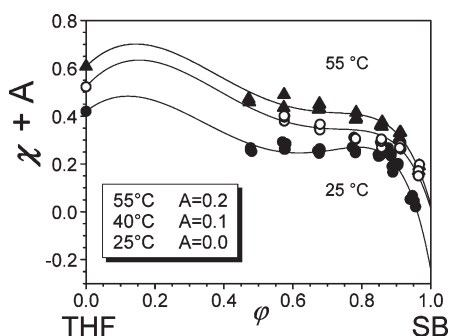


**Figure 6.** Composition dependence of the Flory–Huggins interaction parameter of the system THF/SB. In view of the limited temperature influence on  $\chi$  and on its composition dependence the data are shifted by the indicated additive term.

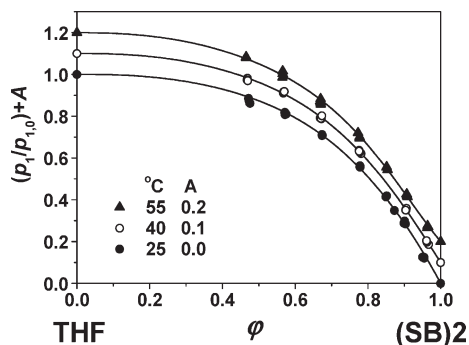


**Figure 7.** Same as Figure 5 but for the system THF/(SB)2.

function of composition for the triblock copolymer (SB)2. The parameter used for the modeling of these curves are presented in Table 7

**THF/(SB)4.** The vapor pressure data for the star shaped block copolymer (SB)4 are shown in Figure 9 and the composition dependencies of  $\chi$  for different temperatures in Figure 10. The parameters used for the modeling of these results are presented in Table 8.

**4.3. Common Analysis.** This section deals with the questions (i) whether some of the parameters of eq 15 modeling block copolymers are interrelated in a similar manner as observed with all other polymer solutions studied so far and (ii) how the composition dependencies of  $\chi$  measured for the block copolymers compare with the corresponding homopolymers.

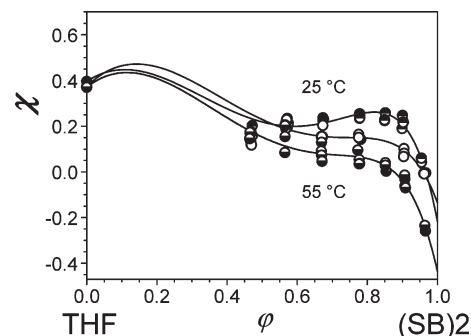


**Figure 8.**  $\chi(\phi)$  for the system THF/(SB)2 (no shift for the different temperatures because the data points are sufficiently different, as distinguished from that of Figure 6).

**Table 7. Characteristic Parameters of Eq 17 and Refractive Index Increments  $dn/dc$  for the System THF/(SB)2**

	25 °C	40 °C	55 °C
$dn/dc$ (mL/g)	0.154	0.170	0.179
$\chi_o$	$0.371 \pm 0.000$	$0.374 \pm 0.000$	$0.371 \pm 0.000$
$\zeta\lambda$	$-1.022 \pm 0.096$	$-1.332 \pm 0.175$	$-1.022 \pm 0.096$
$\nu$	$0.651 \pm 0.017$	$0.601 \pm 0.016$	$0.651 \pm 0.017$
$\tau$	$1.841 \pm 0.039$	$1.901 \pm 0.094$	$1.841 \pm 0.039$

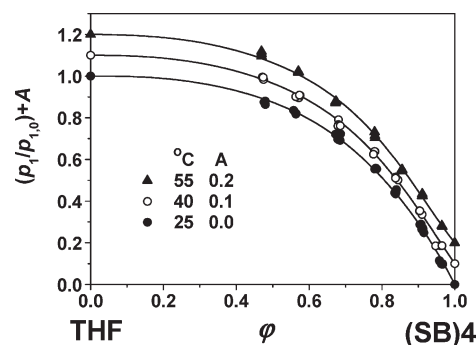


**Figure 9.** Same as Figure 5 but for the system THF/(SB)4.

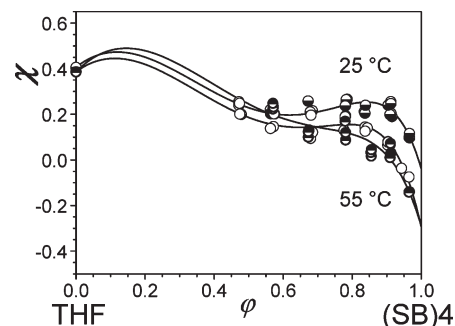


**Figure 10.** Same as Figure 8 but for the system THF/(SB)4.

**Table 8. Characteristic Parameters of Eq 17 and Refractive Index Increments  $dn/dc$  for the System THF/(SB)4**

	25 °C	40 °C	55 °C
$dn/dc$ (mL/g)	0.154	0.163	0.171
$\chi_o$	$0.406 \pm 0.000$	$0.386 \pm 0.000$	$0.386 \pm 0.000$
$\zeta\lambda$	$-0.994 \pm 0.064$	$-0.926 \pm 0.089$	$-1.380 \pm 0.355$
$\nu$	$0.653 \pm 0.012$	$0.667 \pm 0.020$	$0.604 \pm 0.032$
$\tau$	$1.854 \pm 0.031$	$1.800 \pm 0.050$	$1.901 \pm 0.216$

**Interrelation of Parameters.** Within the composition range of pair interactions between the polymers, eq 12 as well as eq 15 reduce to eq 16 specifying how  $\chi_o$  is made up of  $\alpha$

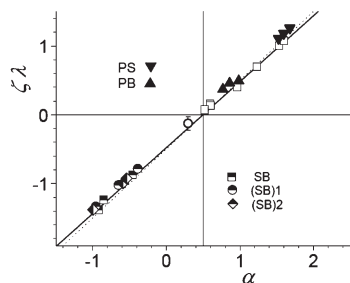


**Figure 11.** Interrelation of the parameters  $\zeta\lambda$  and  $\alpha$  of eq 16. The least-squares fit for all experimental data reads  $\zeta\lambda = 0.958(\alpha - 0.5)$ ; the dotted line corresponds to  $\zeta\lambda = (\alpha - 0.5)$ . Open symbols: data taken for different systems from the literature.<sup>14</sup> Full triangles: THF/PS and THF/PB. Half-filled symbols: THF/block copolymers.

and  $\zeta\lambda$ . The parameter  $\alpha$  measures the effect resulting from the opening of a contact between two segments belonging to different polymer molecules by the insertion of a solvent molecule between them, keeping the conformations of the components identical with their conformations in the pure state. The parameter  $\zeta\lambda$ , on the other hand, quantifies the contribution of the relaxations of the components into their equilibrium state. The fact that the thermodynamic basis of the two consecutive steps of dilution is identical suggests an interrelation between these two parameters. That this is indeed the case is well established for homopolymer solutions and solutions of random copolymers.<sup>27</sup> In Figure 11, we test how the different block copolymers fit into the picture.

The results shown in Figure 11 demonstrate that the data for the block copolymer solutions fall indeed on the same line. There is, however, a fundamental difference concerning their position on this interrelation. Whereas  $\alpha$  is unfavorable (positive) for homopolymers and random copolymers, it is favorable (negative) for the block copolymers. Analogously  $\zeta\lambda$  is favorable in the former case but unfavorable in the latter. In other words “normal” solutions fall almost always into the first quadrant of Figure 11; only for worse than  $\Theta$  conditions  $\alpha$  and  $\zeta\lambda$  become slightly negative (open circle with error bar). In contrast to that, all data for block copolymer solutions are located well inside the third quadrant. According to the present approach the sign of  $\zeta\lambda$  is fixed by the composition dependence of the dimension of the polymer coils. The conformational response is positive, if the coils expand upon dilution as is the case with the solutions of homopolymer in good solvents. Under this condition the volume, which is accessible to the segments belonging to a given macromolecule, increases and the mixing tendency rises. On the other hand,  $\zeta\lambda$  becomes negative if the coils shrink upon dilution. This is for instance the case with homopolymers in worse than  $\Theta$  solvents, because of the high preference of intersegmental contacts over contacts to the solvent, eventually leading to phase separation if it becomes too large. The block copolymers of present interest constitute another example for the shrinkage of polymer coils upon dilution. In this case the deprivation of contacts to like blocks of other macromolecules resulting from the addition of further solvent leads to an “intramolecular demixing”. Why this phenomenon should lead to a reduction of the volume the segments of a given molecule occupy can be rationalized by means of the following simplified consideration: The sum of the volume a random coil of the butadiene block and a random coil of the styrene block occupy should be smaller than the volume of a random coil formed by the entire block copolymer. Considering a solution of polymer concentration  $\phi$  as a *mixed* solvent for the single polymer molecule of interest provides another

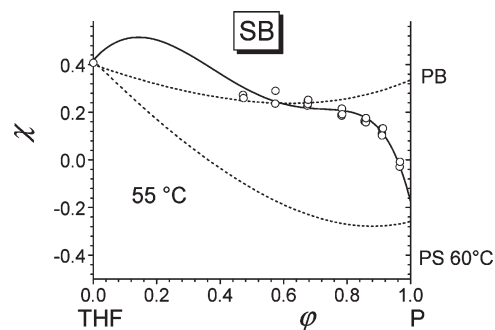


**Figure 12.** Composition dependence of the Flory–Huggins interaction parameter for the system THF/SB (full line) and for THF/PB at 55 °C; the information for THF/PS (ref 27) refers to 60 °C.

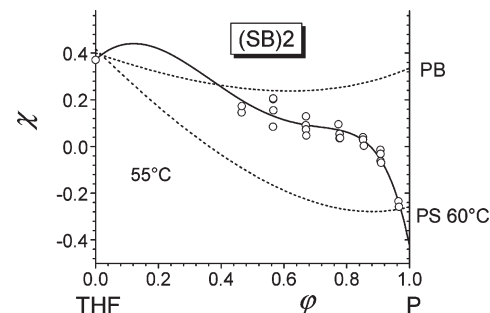


**Figure 13.** Like Figure 12 but for (SB)2.

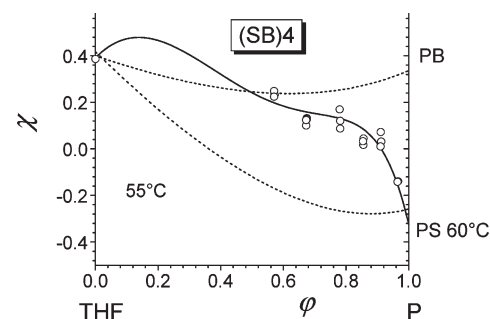


**Figure 14.** Like Figure 12 but for (SB)4.

opportunity to explain the influences of polymer concentration on the changes in coil dimension. Adding further solute molecules to a homopolymer solution in a poor solvent leads to an expansion because of the establishment of favorable contacts between the segment of a given macromolecules with the segments of other polymer macromolecules. For the block copolymer solutions, the same reasoning holds true. In this case unfavorable contacts between the two types of segments of a single macromolecules can now be substituted by interaction with like segments of other polymer molecules.

**Comparison of the Block Copolymers with the Corresponding Homopolymers.** The following three graphs (Figures 12–14) show the composition dependent interaction parameters for the three types of block copolymers with THF, together with that of polybutadiene and of polystyrene with the same solvent for 55 °C.

The most striking feature of these three graphs is the absence of fundamental differences between the solution behavior of the block copolymers of different structure. All  $\chi(\phi)$  dependencies start for dilute solutions very close to the  $\chi_o$  values of the two homopolymers; upon an augmentation of  $\phi$  they pass a maximum and approach  $\chi$  values in the limit of  $\phi \rightarrow 1$  which are either very close to  $\chi_{\text{THF/PS}}$  or even lower.

Furthermore, the heats of dilutions are also very similar for all block copolymers: on the dilute side they are close to athermal, whereas they become pronouncedly endothermal as the polymer concentration increases.

In order to rationalize these observations we discuss the molecular processes that should take place upon the addition of solvent, because  $\chi$  constitutes the reduced residual Gibbs energy of dilution. Keeping in mind that the number of contacts between butadiene (B) and styrene (S) segments is minimized in the melt by “demixing” into microphases and the establishment of an adequate morphology. In this manner the adverse contacts between B and S are almost exclusively confined to the interphases. In view of this situation it is reasonable to assume that solvent molecules added to such a melt will preferentially open these B–S contacts, because this process will lead to the maximum reduction in the Gibbs energy of the system. Further addition of solvent will increasingly also open B–B and S–S contacts, but also generate new B–S contacts because of the spatial expansion of the interphase into which more and more polymer molecules, initially located inside the microphases, will be transferred. This means that  $\chi$  should gradually ascend upon dilution, as is actually the case.

Once the microphase separation is overcome by dilution, one would expect the curve for the copolymer to be located between the two curves representing the homopolymer and to increase smoothly. This is however not the case as demonstrated by the maxima in  $\chi(\phi)$ . One might speculate that the reason for this behavior lies in the appearance of a new mode of evading unfavorable B–S contacts, namely via intramolecular segregation of these units. This idea leads us to the assumption that the number of such adverse intersegmental contacts is largest at the composition of the maximum because the evasion to the microphases has lost importance and the coil overlap is still too high for the intramolecular segregation to become operative. Once the maximum is surpassed the latter effect dominates and leads to the observed reduction of  $\chi$ .

## 5. Conclusions

The Flory–Huggins interaction parameters obtained from vapor pressure and light scattering measurements for the solutions of the different block copolymers in THF—a solvent which is favorable for the B blocks as well as for the S blocks—are very similar to each other in their magnitude and composition dependence, irrespective of their particular molecular architecture. In all cases  $\chi(\phi)$  passes a maximum and the heats of dilution are close to athermal at low  $\phi$  values but become pronouncedly endothermal for high polymer concentrations.

The modeling of these results by means of series expansions of  $\chi$  with respect to  $\phi$  (like Redlich–Kister) yields unsatisfactory results only. An approach subdividing the dilution process into two steps, where the second step accounts for chain connectivity and conformational relaxation of polymers, on the other hand, enables a consistent modeling of the data. This capability is attributed to the fact that the second step quantifies the contributions of nonrandom mixing to the Flory–Huggins interaction parameter. A detailed analysis of the data reveals fundamental differences in the reasons why a certain solvent is favorable for a homopolymer or for a block copolymer. In the former case, it is a favorable second step of dilution which dominates, whereas it is a favorable first step in the case of the

block copolymers. The maxima in  $\chi(\phi)$  solvent/block copolymer systems are tentatively attributed to a change in the molecular mechanisms enabling the avoidance of unfavorable contacts between the chemically different blocks. At high  $\phi$  values, it is the microphase separation which minimizes such encounters, whereas intramolecular segregation becomes active at high dilution. Within some composition range of transition the possibilities to “shield” the blocks from each other become worst and  $\chi$  passes its maximum.

In this work we have only investigated the solution behavior of block copolymers in a solvent which is favorable for both blocks. These results cannot be expected to hold true for systems where the solvent is favorable for one block but marginal for the other. For further investigations, it would therefore be interesting to expand the experiments to preferential solvents.

**Acknowledgment.** X.X. gratefully acknowledges the National Natural Science Foundation of China (No. 20844006).

## References and Notes

- (1) Legge, N. R.; Holden, G.; Schroeder, H. E. In *Thermoplastic elastomers: A comprehensive review* Hanser: New York, 1987.
- (2) Bates, F. S.; Fredrickson, G. H. *Annu. Rev. Phys. Chem.* **1990**, *41*, 525.
- (3) Fredrickson, G. H.; Bates, F. S. *Annu. Rev. Mater. Sci.* **1996**, *26*, 501–550.
- (4) Ruzette, A.-V.; Leibler, L. *Nat. Mater.* **2005**, *4*, 19–31.
- (5) Matsen, M. W. *J. Phys.: Condens. Matter* **2002**, *14*, R21–R47.
- (6) Haryono, A.; Binder, W. H. *Small* **2006**, *2*, 600–611.
- (7) Bates, F. S. *Science* **1991**, *251*, 898–905.
- (8) Abetz, V.; Simon, P. F. W. *Adv. Polym. Sci.* **2005**, *189*, 125–212.
- (9) Li, M. Q.; Coenjarts, C. A.; Ober, C. K. *Block Copolym. II* **2005**, *190*, 183–226.
- (10) Alexandridis, P.; Spontak, R. J. *Curr. Opin. Colloid Interface Sci.* **1999**, *4*, 130–139.
- (11) Huang, W.; Luo, C.; Li, B.; Han, Y. *Macromolecules* **2006**, *39*, 8075–8082.
- (12) Xiong, X. P.; Eckelt, J.; Wolf, B. A.; Zhang, Z. J.; Zhang, L. *J. Chromatogr. A* **2006**, *1110*, 53–60.
- (13) Bercea, M.; Cazacu, M.; Wolf, B. A. *Macromol. Chem. Phys.* **2003**, *204*, 1371–1380.
- (14) Wolf, B. A. *Macromol. Chem. Phys.* **2003**, *204*, 1381–1390.
- (15) Gurevich, I. G.; Gisina, K. B.; Shchitnikov, V. K.; Dubasova, V. S.; Nilonov, V. L. *J. Eng. Phys. Thermophys.* **1982**, *42*, 304.
- (16) Stryuk, S.; Wolf, B. A. *Macromolecules* **2005**, *38*, 812–817.
- (17) Petri, H. M.; Schuld, N.; Wolf, B. A. *Macromolecules* **1995**, *28*, 4975–4980.
- (18) Barth, C.; Horst, R.; Wolf, B. A. *J. Chem. Thermodyn.* **1998**, *30*, 641–652.
- (19) Bodmann, O. *Chem. Ing. Tech.* **1957**, *7*, 468–473.
- (20) Redlich, O.; Kister, A. T. *Ind. Eng. Chem.* **1948**, *40*, 345–348.
- (21) Jouyban, A.; Chew, N. Y. K.; Chan, H. K.; Sabour, M.; Acree, W. E. *Chem. Pharm. Bull.* **2005**, *53*, 634–637.
- (22) Du, Z. M.; Jiang, Z. Q.; Li, C. R. *J. Alloys Compd.* **2007**, *427*, 148–152.
- (23) Iloukhani, H.; Rostami, Z. *J. Chem. Eng. Data* **2007**, *52*, 921–928.
- (24) Kharat, S. J.; Nikam, P. S. *J. Mol. Liq.* **2007**, *131*, 81–86.
- (25) Bercea, M.; Wolf, B. A. *Macromol. Chem. Phys.* **2006**, *207*, 1661–1673.
- (26) Eckelt, J.; Sugaya, R.; Wolf, B. A. *Biomacromolecules* **2008**, *9*, 1691–1697.
- (27) Bercea, M.; Eckelt, J.; Wolf, B. A. *Ind. Eng. Chem. Res.* **2009**, *48*, 4603–4606.
- (28) Ocando, C.; Tercjak, A.; Serrano, E.; Ramos, J. A.; Corona-Galvan, S.; Parellada, M. D.; Fernandez-Berridi, M. J.; Mondragon, I. *Polym. Int.* **2008**, *57*, 1333–1342.
- (29) Wang, J. F.; Muller, M.; Wang, Z. G. *J. Chem. Phys.* **2009**, *130*, 154902.